Int. J. Bio-Inorg. Hybr. Nanomater., 4(3): 121-128, Autumn 2015

# Thiol-functionalized mesoporous silica as nanocarriers for anticancer drug delivery

*Z. Bahrami[1*]; A. Badiei[2]; Gh. Mohammadi Ziarani[3]*

[1] *Faculty of Nanotechnology, Semnan University, Semnan, Iran*
[2] *School of Chemistry, College of Science, University of Tehran, Tehran, Iran*
[3] *Research Laboratory of Pharmaceutical, Alzahra University, Tehran, Iran*

Received: 27 April 2015; Accepted: 30 June 2015

**ABSTRACT:** The present study deals with the synthesis andfunctionalization of mesoporous silica nanoparticles as drug delivery platforms. SBA-15 nanorods with high surface area (1010 $m^2g^{-1}$) were functionalized by post grafting method using 3-mercaptopropyl trimethoxysilane (MPTS). The parent and thiol-functionalized SBA-15 nanorods were used as nanocarriers for an anticancer drug (gemcitabine). The characterization of all samples were done by small angle X-ray scattering (SAXS), $N_2$ adsorption/desorption, scanning electron microscopy (SEM), transmission electron microscopy (TEM), FTIR and UV spectroscopies. The adsorption and release properties of all samples were investigated. It was found that the surface functionalization increases the interaction between the carrier and gemcitabine and results in the loading enhancement of the drug. The obtained results reveal that the surface functionalization leads towards significant decrease of the drug release rate. These findings demonstrate that the functionalized mesoporous system is appropriate drug delivery platform due to their loading content and the possibility to modify drug release.

**Keywords:** *Anticancer; Gemcitabine; Nanorods; SBA-15; Thiol-functionalization*

## INTRODUCTION

Recently, mesoporous silica nanoparticles (MSNs) have been emerged as drug delivery systems (DDS) because of several unique properties such as high surface area, large pore volume, uniform and tunable pore sizes, very high thermal and chemical stability, controllable morphology, modifiable surfaces, lack of toxicity and well biocompatibility (Vallet-Regi, *et al.*, 2001, Tourne-Peteilh, *et al.*, 2003, Doadrio, *et al.*, 2006, Prokopowicz and Przyjazny 2007, Nunes, *et al.*, 2007).

The porous system architecture, thickness of walls, chemical modification of the surface, chemical characteristics of the adsorbed drug, morphology of mesoporous silica particles and many other parameters can influence on the drug loading and release into and out of MSNs (Tozuka, *et al.*, 2010, Izquierdo-Barba, *et al.*, 2005, Munoz, *et al.*, 2003, Song, *et al.*, 2005, Heikkila, *et al.*, 2007). It was demonstrated that the surface modification with appropriate functional groups is an important method of varying the drug loading and release properties of mesoporous silica materials. For example, MSNs modified with amine groups were applied as

(*) Corresponding Author - e-mail: bahrami.zoh@semnan.ac.ir

carriers for adsorption of drugs with acidic character (Halamova, *et al.*, 2010). In contrary, modification of the surface with acids (e.g. with carboxylic groups) increases the adsorptive properties of drugs with basic properties (Doadrio, *et al.*, 2004). Several research groups investigated the effect of the morphology of MSNs on the drug adsorption and release. Tsai, *et al.* found that rod-like MSNs have greater potential than that of spherical ones in monitoring the cell trafficking, cancer cell metastasis, and drug/DNA delivery (Tsai, *et al.*, 2008).SBA-15 with highly ordered 2D-hexagonal mesostructure with large pore size of 4.6–10.0 nm is attractive for the easy modification and application as drug delivery system. The performance improvement of SBA-15 particles affected by their size and morphology. The rod-like morphology of SBA-15 is more interesting due to its small dimensions, which results in short diffusion paths and therefore the possibility of fast adsorption and mass transfer (Lai, *et al.*, 2003, Qu, *et al.*, 2006, Tang, *et al.*, 2006).

Gemcitabine (Gem) (Fig. 1) is a water-soluble low-molecular-weight anticancer drug that is commonly used for the treatment of several kinds of cancers including colon, pancreatic, lung, breast, ovarian, and bladder. Different drug delivery systems such as liposomes and polymeric nanoparticles were designed in order to protect Gem from rapid metabolization, overcome drug resistance, target drug delivery, and improving its anticancer efficacy (Braakhuis, *et al.*, 1991, Burris and Storniolo 1997, Patra, *et al.*, 2010, Sevimli and Yilmaz 2012).

This paper describes the adsorption and release of gemcitabine on the thiol-functionalized SBA-15 nanorods. Investigation of the effect of the surface functionalization on the adsorption capacity and release behavior of Gem is the main aim of this study.

## MATERIALS AND METHODS

### *Materials*

Poly (ethylene glycol) block poly (propylene glycol) block poly (ethylene glycol), P123, ($EO_{20}PO_{70}EO_{20}$, $M_W$ = 5800 g/mol) was obtained from Aldrich. Tetraethyl orthosilicate (TEOS), hydrochloric acid (35 %), ethanol and 3-mercaptopropyl trimethoxysilane (MPTS) were purchased from Merck. Gemcitabine was obtained from Lilly France S.A.S. Company. All chemical reagents were used without further purification.

### *Synthesis of SBA-15 nanorods*

SBA-15 nanorods were synthesized according to the procedure that described in our previous work (Bahrami, *et al.*, 2014). In a typical synthesis, 23.4 g of non-ionic triblock copolymer (Pluronic P123) was dissolved in the mixture of deionized water (606.8 g) and hydrochloric acid (146.4 g, 35 %). Then, 50 g of TEOS was added to this clear solution while stirring at the rate of 500 rpm at 55°C. The reaction batch was maintained at static conditions for 24 h (hydrolysis time) at this temperature and then for another 24 h at 100°C for further condensation. The precipitate was obtained after filtration, and ethanol extraction. A soxhlet extractor was used for removing the triblock copolymer template.

### *Preparation of thiol-functionalized SBA-15 nanorods (SH-SBA-15)*

To functionalize the surface of SBA-15 nanorods with mercapto groups, 0.1 g of SBA-15 nanorods was dispersed in 20 mL of anhydrous ethanol. Following the addition of 3-mercaptopropyl trimethoxysilane (MPTS) (1 mL), the mixture was stirred moderately at

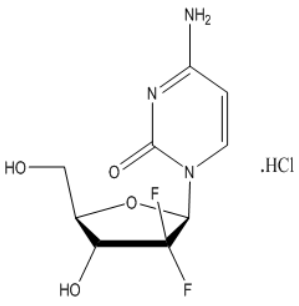


Fig. 1: Chemical structure of gecitabine

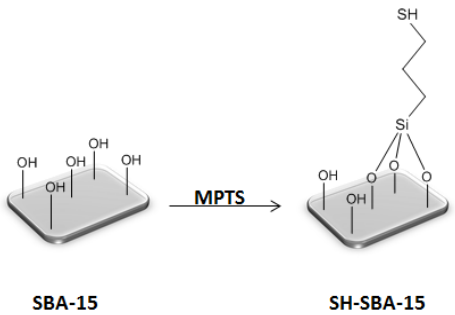


Fig. 2: Thiol-functionalization of SBA-15 nanorods

80°C for 6 h. The precipitate was collected by centrifugation, washed with ethanol and dried at room temperature to give the thiol-functionalized SBA-15 nanorods as white powder. The obtained modified sample was denoted as SH-SBA-15 (Fig. 2).

***Adsorption of gemcitabine on SBA-15 nanocarriers***

20 mg of the non-modified or thiol-functionalized SBA-15 nanorods was dispersed in 8 mL of gemcitabine solution (2.5 mg $mL^{-1}$). The mixture was stirred at room temperature for 24 h in order to load Gem on SBA-15 nanorods. The gemcitabine-loaded samples were collected by centrifugation and rinsed several times with distilled water to remove the physically adsorbed Gem. The prepared samples were labeled as G@SBA-15 and G@SH-SBA-15. UV/Vis spectrophotometer was used to measure the amount of the loaded drug at the wavelength of 269 nm. The drug loading content and the entrapment efficiency were calculated using the following equations:

$$\text{Loading content}(\%) = \left(\frac{\text{Weight of Gem in mesoporous material}}{\text{Weight of Gem loaded mesoporous material}}\right) \times 100$$

$$\text{Entrapment efficiency}(\%) = \left(\frac{\text{Weight of Gem in mesoporous material}}{\text{Initial weight of Gem}}\right) \times 100$$

***Gemcitabine release***

Phosphate-buffered saline (PBS) solutions with the pH values of 5.6 and 7.4 were chosen for the drug release experiments. The certain amount of Gem-loaded samples was suspended in 4 mL of PBS solutions. The solution was kept at 37°C using an incubator in order to simulate body temperature. At scheduled time points, suspension was centrifuged at 13000 rpm for 15 min. The amount of released drug was measured by a UV/Vis spectrophotometer at the wavelength of 269 nm. The measurement was repeated three times for each sample to ensure the accuracy.

***Instrumentation***

The small angle X-ray scattering (SAXS) patterns were recorded with a model Hecus S3-MICROpix SAXS diffractometer with a one-dimensional PSD detector using Cu Kα radiation (50 kV, 1 mA) at the wavelength 1.542 Å. The SEM and transmission electron microscopy (TEM) images were taken using Oxford LEO 1455 V STEM and Philips EM-208 100 kV, respectively. Nitrogen physisorption isotherms were obtained on a BELSORP mini-II at liquid nitrogen temperature (77 K). The specific surface areas were measured using multiple point Brunauer–Emmett–Teller method. The pore size distributions were calculated using desorption branches of the isotherms by Barrett–Joyner–Halenda (BJH) method. The FTIR spectra were recorded using Equinox 55 spectrometer in the range between 400 and 4000 $cm^{-1}$. The UV/Vis absorption spectra were recorded using a Ray light, UV 1600 spectrophotometer.

## RESULTS AND DISCUSSION

***Small angle X-ray scattering analysis (SAXS)***

The SAXS patterns of the non-modified and thiol-functionalized SBA-15 nanorods were displayed in Fig. 3. All the samples have a single intensive reflection at around $2\theta = 0.72°$ and two additional peaks related to the higher ordering (110) and (200) reflections similar to the typical SBA- 15 materials, that is reported in the literature (Bahrami, *et al.*, 2015a). These three peaks are characteristic of the ordered structure of hexagonal lattice (Bahrami, *et al.*, 2015b). The existence of three main diffraction peaks in the patterns of the functionalized sample confirms that the introduction of the organic functionalities does not destroy the mesoporous structure of the parent SBA-15. However, due to the existence of organic groups in the mesochannels, a decrease in the intensity of peaks is observed.

***Morphology study***

The scanning electron microscopy (SEM) image of SBA-15 matrix (Fig. 4a) is shown that the synthesized particles having rod-like shape. As it can be observed in the transmission electron microscopy (TEM) image (Fig. 4b), the width and length of these rods are about 100 nm and 1 μm, respectively. In addition, these nanorods have highly ordered 2D-hexagonal mesochannels along the length of the rods.

***Nitrogen adsorption/desorption analysis***

$N_2$ adsorption/desorption measurements of the non-modified SBA-15 nanorods, thiol-functionalized and

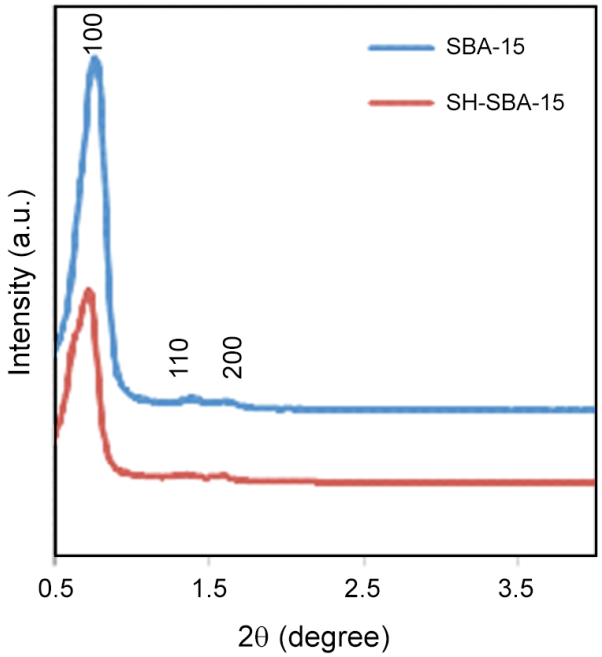


Fig. 3: SAXS patterns of SBA-15 nanorods and SH-SBA-15 sample

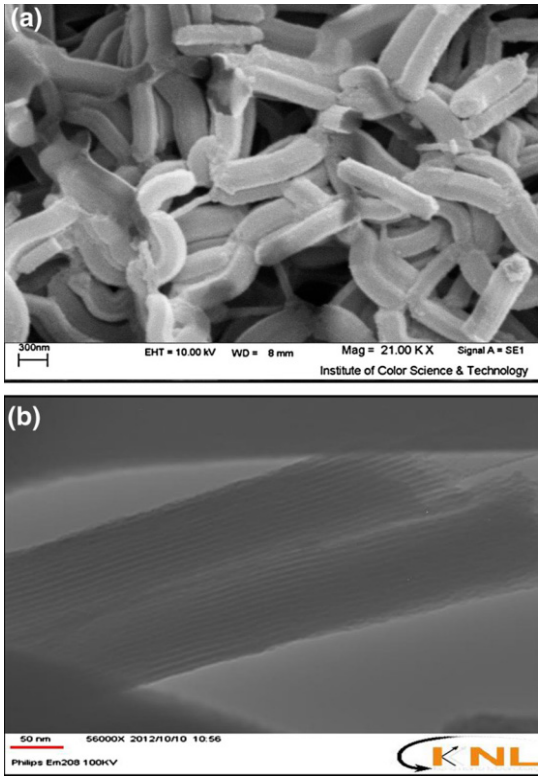


Fig. 4: (a) SEM and (b) TEM images of SBA-15 nanorods

Gem-loaded samples exhibiting a similar trend. A typical irreversible type IV nitrogen adsorption isotherm with an H1 hysteresis loop were observed for the all samples (Fig. 5a) (Horcajada, *et al.*, 2004). The shape and the position of hysteresis loop (at $p/p_0$ from 0.60 to 0.85) indicate cylindrical mesopores with very narrow pore size distributions (Andersson, *et al.*, 2004). The lower amount of the adsorbed nitrogen and the shift of hysteresis loop of the functionalized and Gem loaded samples toward lower relative pressures are the indication of the presence of organic functionalities groups and drug molecules in the pores. The textural properties of the all samples are summarized in Table 1. As it can be observed, there is a decreasing trend in the specific surface area ($S_{BET}$), pore volume ($V_p$), and pore diameter ($D_p$) after the surface functionalization and drug loading. The pore size distribution was calculated by BJH method based on the desorption branch of $N_2$ adsorption/desorption isotherms. It is observed that all of the samples have narrow pore size distribution with uniform mesochannels (Fig. 5b).

### *FTIR measurement*

Infrared spectra of the SBA-15 nanorods, thiol-functionalized and the Gem loaded samples were illustrated in Fig. 6. For all samples, the band at around 3400 $cm^{-1}$ can be assigned to the stretching vibration of Si-OH groups. The stretching vibrations of Si-O-Si

Table 1: Specific surface area (SBET) ($m^2g^{-1}$), pore volume ($V_p$) ($cm^3g^{-1}$) and pore diameter ($D_p$) (nm) from $N_2$ adsorption/desorption for SBA-15 nanorods, thiol-functionalized and Gem loaded samples

| samples | Textural properties | | |
|---|---|---|---|
| | $S_{BET}$ ($m^2g^{-1}$) | $V_p$($cm^3g^{-1}$) | $D_p$ (nm) |
| SBA-15 nanorods | 1010 | 1.27 | 7.06 |
| SH-SBA-15 | 598 | 1.02 | 5.40 |
| G@SBA-15 nanorods | 449 | 0.811 | 6.18 |
| G@SH-SBA-15 | 358 | 0.826 | 5.40 |

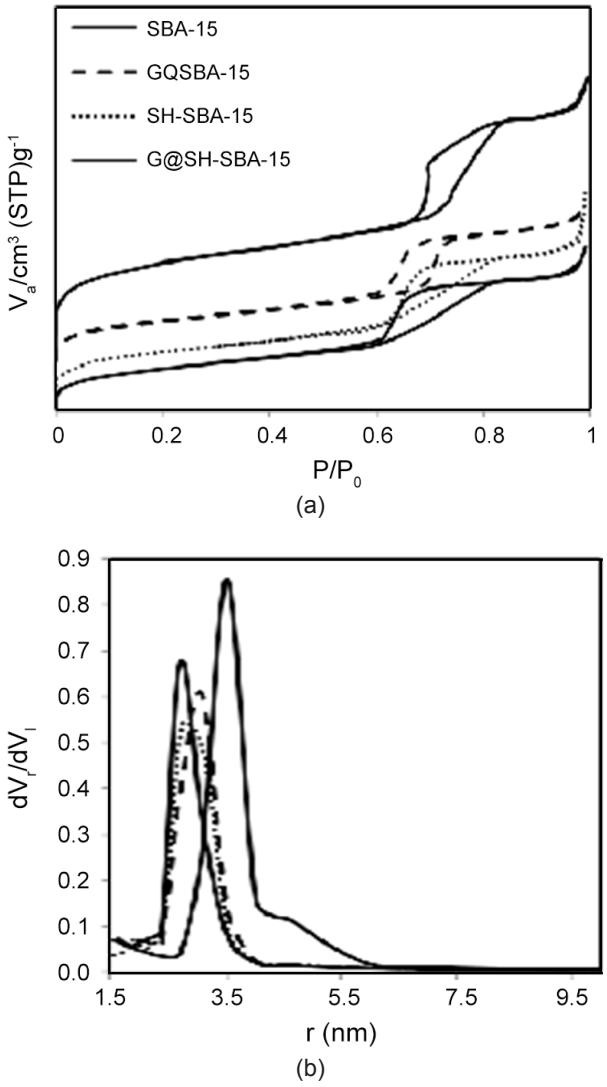


Fig. 5: (a) $N_2$ adsorption/desorption isotherms and (b) pore size distribution of SBA-15 nanorods, thiol-functionalized and Gem loaded samples

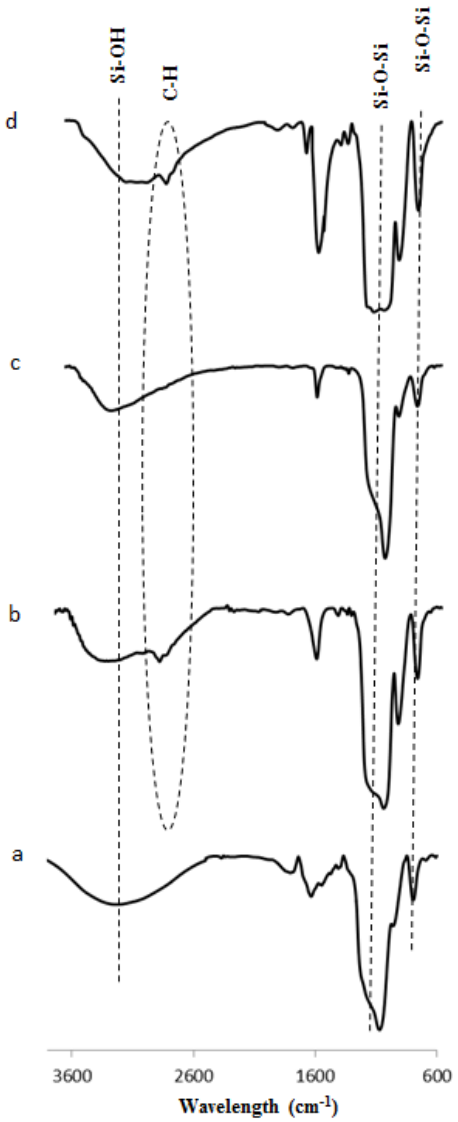


Fig. 6: FTIR spectra of (a) SBA-15 nanorods, (b) SH-SBA-15, (c) G@SBA-15 and (d) G@SH-SBA-15

appear as two peaks: one broad and strong peak centered at around 1100 cm$^{-1}$; one narrow and relatively weak peak near 800 cm$^{-1}$ (Bahrami, *et al.*, 2015b). In addition, the small peaks observed at around 2800 and 2900 cm$^{-1}$ result from the CH stretching vibrations. Although, the characteristic peak (related to the –SH groups) could not be observed at around 2580 cm$^{-1}$ due to the sample containing trace amounts of the mercaptopropyltrimethoxysilane(Qu, *et al.*, 2006). The new adsorption band is observed in the spectra of Gem loaded samples. The peak at around 1480 cm$^{-1}$ is due to N-H bending of Gem molecules (Bahrami, *et al.*, 2014). These results indicate that the Gem loading was done successfully.

Table 2: Gemcitabine loading content and entrapment efficiency of the non-modified and thiol-functionalized SBA-15 nanorods

| Gem loaded samples | Loading content (%) | Entrapment efficiency (%) |
|---|---|---|
| G@SBA-15 nanorods | 7 | 7.90 |
| G@SH-SBA-15 | 12.96 | 14.90 |

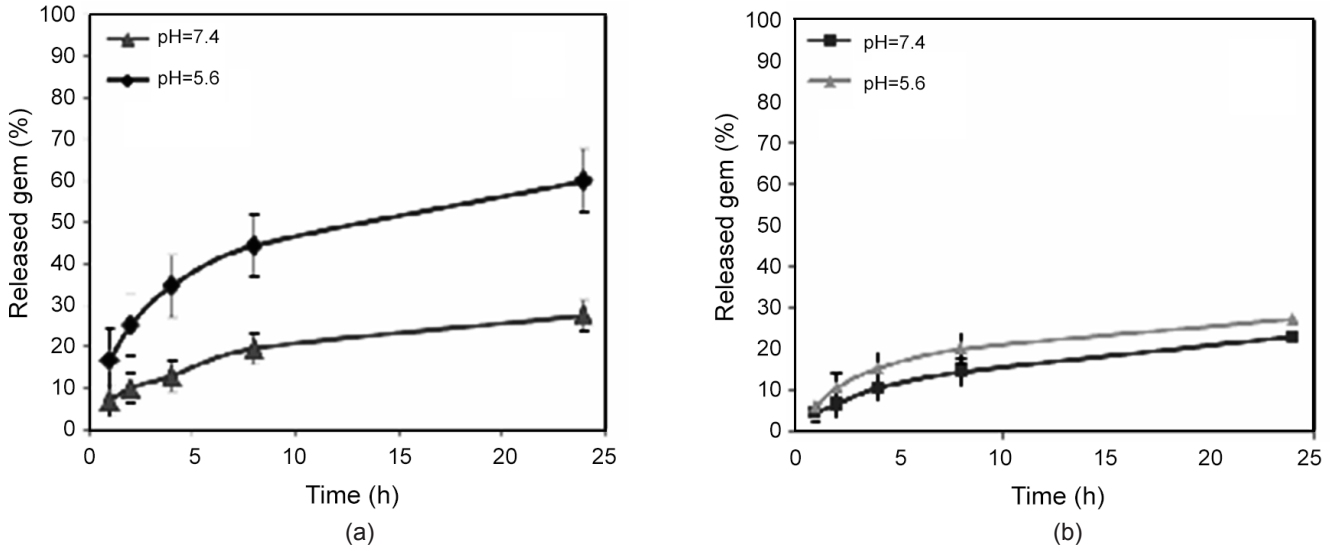


Fig. 7: Release profiles of (a) G@SBA-15 nanorods and (b) G@SH-SBA-15

***Gemcitabine loading and release***

Successful modification was also evidenced by the drug adsorption experiments. The amount of adsorbed gemcitabine of the non-modified and thiol-functionalized SBA-15 nanorods was displayed in Table 2. It was found that the non-modified SBA-15 nanorods can adsorb 7 wt.% of Gem. In contrast, the surface modification resulted in higher amount of adsorbed Gem. This is due to increasing the interaction between the carrier and the drug.

The results of the gemcitabine release from the Gem loaded samples are plotted in Fig. 7. The drug release behaviour was studied in PBS buffers with different pH values of 5.6 and 7.4 at 37°C. As shown, in contrast with G@SBA-15, slower release rate was observed from the thiol-functionalized sample. This fact could be explained by taking into account that the interaction between Gem and the functionalized sample is stronger than that of between Gem and silanol groups of the non-modified SBA-15 nanorods. Therefore, by controlling the surface properties of SBA-15 nanorods it should be possible to prepare novel drug carriers with the desired release rate.

## CONCLUSIONS

In the present work, the non-modified and thiol-functionalized SBA-15 nanorods were used as the carriers for the adsorption and release of anticancer drug such as gemcitabine. The surface functionalization leads towards formation of the carriers that have strong interaction with the drug. In contrast with SBA-15 nanorods, the drug release rate of the thiol-functionalized sample is not pH dependent. In addition, slower release rate was observed from this functionalized sample. Therefore, it is demonstrated that the thiol-functionalized SBA-15 nanorods can be suitable carriers for gemcitabine. The obtained results give promising perspectives for future application of mesoporous materials in drug delivery systems.

## ACKNOWLEDGMENT

The authors thank the financial support from the University of Tehran.

## REFERENCES

Andersson, J.; Rosenholm, J.; Areva, S.; Linden, M., (2004). Influences of Material Characteristics on Ibuprofen Drug Loading and Release Profiles from Ordered Micro- and Mesoporous Silica Matrices. Chem. Mater., 16: 4160-4167.

Bahrami, Z.; Badiei, A.; Atyabi, F., (2014). Surface Functionalization of SBA-15 Nanorods for Anti-

cancer Drug Delivery. Chem. Eng. Res. Des., 92: 1296-1303.

Bahrami, Z.; Badiei, A.; Atyabi, F.; Darabi, H.R.; Mehravi, B., (2015a). Piperazine and its Carboxylic acid Derivatives-functionalized Mesoporous Silica as Nanocarriers for Gemcitabine: Adsorption and Release Study. Mate. Sci. Eng. C, 49: 66-74.

Bahrami, Z.; Badiei, A.; Ziarani, G.M., (2015b). Carboxylic acid-functionalized SBA-15 Nano rods for Gemcitabine Delivery. J. Nanopart. Res., 17: 125-137.

Braakhuis, B.J.; Dongen, G.A.V.; Vermorken, J.B.; Snow, G.B., (1991). Preclinical in Vivo Activity of 2′, 2′- difluorodeoxycytidine (Gemcitabine) Against Human Head and Neck Cancer. Cancer Res., 51: 211-214.

Burris, H.; Storniolo, A.M., (1997). Assessing Clinical Benefit in the Treatment of Pancreas Cancer: Gemcitabine Compared to 5-fluorouracil. Eur. J. Cancer, 33: S18-S22.

Doadrio, A.L.; Sousa, E.M.; Doadrio, J.C.; Perez Pariente, J.; Izquierdo-Barba, I. Vallet-Regi, M., (2004). Mesoporous SBA-15 HPLC Evaluation for Controlled Gentamicin Drug Delivery. J Control Release, 97: 125-32.

Doadrio, J.C.; Sousa, E.M.B.; Izquierdo-Barba, I.; Doadrio, A.L.; Perez-Pariente, J. Vallet-Regi, M., (2006). Functionalization of Mesoporous Materials with Long Alkyl Chains as a Strategy for Controlling Drug Delivery Pattern. J. Mate. Chem., 16: 462-466.

Halamova, D.; Badanicova, M.; Zelenak, V.; Gondova, T.; Vainio, U., (2010). Naproxen Drug Delivery Using Periodic Mesoporous Silica SBA-15. Appl. Surf. Sci., 256: 6489-6494.

Heikkila, T.; Salonen, J.; Tuura, J.; Hamdy, M.S.; Mul, G.; Kumar, N.; Salmi, T.; Murzin, D.Y.; Laitinen, L.; Kaukonen, A.M.; Hirvonen, J.; Lehto, V.P., (2007). Mesoporous Silica Material TUD-1 as a Drug Delivery System. Int. J. Pharm, 331: 133-138.

Horcajada, P.; Ramila, A.; Perez-Pariente, J.; Vallet Regı, M., (2004). Influence of Pore Size of MCM-41 Matrices on Drug Delivery Rate. Microporous Mesoporous Mater., 68: 105-109.

Izquierdo-Barba, I.; Martinez, A.; Doadrio, A.L.; Perez-Pariente, J.; Vallet-Regi, M., (2005). Release Evaluation of Drugs from Ordered Three-dimensional Silica Structures. Eur. J. Pharm. Sci., 26: 365-373.

Lai, C.Y.; Trewyn, B.G.; Jeftinija, D.M.; Jeftinija, K.; Xu, S.; Jeftinija, S. Lin, V.S.Y., (2003). J. Am. Chem. Soc., 125: 4451.

Munoz, B.; Ramila, A.; Perez-Pariente, J.; Diaz, I.; Vallet-Regi, M., (2003). MCM-41 Organic Modification as Drug Delivery Rate Regulator. Chem. Mater., 15: 500.

Nunes, C.D.; Vaz, P.D.; Fernandes, A.C.; Ferreira, P.; Romao, C.C.; Calhorda, M.J., ( 2007). Loading and Delivery of Sertraline Using Inorganic Micro and Mesoporous Materials. Eur. J. Pharm Biopharm., 66: 357-365.

Patra, C.R.; Bhattacharya, R.; Mukhopadhyay, D.; Mukherjee, P., (2010). Fabrication of Gold Nanoparticles for Targeted Therapy in Pancreatic Cancer. Adv. Drug. Deliv. Rev., 62: 346-61.

Prokopowicz, M.; Przyjazny, A., (2007). Synthesis of Sol-gel Mesoporous Silica Materials Providing a Slow Release of Doxorubicin. J. Microencapsul, 24: 694-713.

Qu, F.; Zhu, G.; Huang, S.; Li, S.; Sun, J.; Zhang, D.; Qiu, S., (2006). Controlled Release of Captopril by Regulating the Pore Size and Morphology of Ordered Mesoporous Silica. Microporous Mesoporous Mater., 92: 1-9.

Sevimli, F.; Yılmaz, A., (2012). Surface Functionalization of SBA-15 Particles for Amoxicillin Delivery. Microporous Mesoporous Mater., 158: 281-291.

Song, S.W.; Hidajat, K.; Kawi, S., (2005). Functionalized SBA-15 Materials as Carriers for Controlled Drug Delivery: Influence of Surface Properties on Matrix−Drug Interactions. Langmuir, 21: 9568-9575.

Tang, Q.; Xu, Y.; Wu, D.; Sun, Y.,(2006). A Study of Carboxylic-modified Mesoporous Silica in Controlled Delivery for Drug Famotidine. J. Solid State Chem., 179: 1513-1520.

Tourne-Peteilh, C.; Lerner, D.A.; Charnay, C.; Nicole, L.; Begu, S.; Devoisselle, J.M., (2003). The Potential of Ordered Mesoporous Silica for the Storage of Drugs: The Example of a Pentapeptide

Encapsulated in a MSU-Tween 80. Chem. Phys. Chem., 4: 281-286.

Tozuka, Y.; Sugiyama, E.; Takeuchi, H., (2010). Release Profile of Insulin Entrapped on Mesoporous Materials by Freeze-thaw Method. Int. J. Pharm., 386: 172-177.

Tsai, C.P.; Hung, Y.; Chou, Y.H.; Huang, D.M.; Hsiao, J.K.; Chang, C.; Chen, Y.C.; Mou, C.Y., (2008). High-Contrast Paramagnetic Fluorescent Mesoporous Silica Nanorods as a Multifunctional Cell-Imaging Probe. Small, 4: 186-191.

Vallet-Regi, M.; Ramila, A.; Real, R.P.d.; Perez-Pariente, J., (2001). A New Property of MCM-41: Drug Delivery System. Chem. Mater., 13: 308-311.

## AUTHOR (S) BIOSKETCHES

**Zohreh Bahrami**, Assistant Professor, Faculty of Nanotechnology, Semnan University, Semnan, Iran. *E-mail: bahrami.zoh@semnan.ac.ir*

**Alireza Badiei**, Professor, School of Chemistry, College of Science, University of Tehran, Tehran, Iran

**Ghodsi Mohammadi Ziarani**, Professor, Research Laboratory of Pharmaceutical, Alzahra University, Tehran, Iran